Biomaterials Science

Sequestering Survivin to functionalized nanoparticles: A strategy to enhance apoptosis in cancer cells

Journal:	*Biomaterials Science*
Manuscript ID	BM-ART-12-2015-000580.R1
Article Type:	Paper
Date Submitted by the Author:	26-Jan-2016

Complete List of Authors:	Jenkins, Ragini; Clemson University, Materials Science and Engineering Bandera, Yuriy; Clemson University, Materials Science and Engineering Daniele, Michael; Clemson University, Materials Science and Engineering Ledford, LeAnna; Clemson University, Genetics and Biochemistry Tietje, Ashlee; Clemson University, Biological Sciences Kelso, Andrew; Clemson University, Genetics and Biochemistry Sehorn, Michael; Clemson University, Genetics and Biochemistry Wei, Yanzhang; Clemson University, Biological Sciences Chakrabarti, Mrinmay; University of South Carolina School of Medicine,, Pathology, Microbiology, and Immunology Ray, SK ; University of South Carolina School of Medicine, Pathology, Microbiology, and Immunology Foulger, Stephen; Clemson University, Materials Science and Engineering

SCHOLARONE™
Manuscripts

Journal Name

ARTICLE TYPE

Cite this: DOI: 10.1039/xxxxxxxxxx

Sequestering survivin to functionalized nanoparticles: A strategy to enhance apoptosis in cancer cells†

Ragini Jenkins,[a] Yuriy P. Bandera,[a] Michael A. Daniele,[a] LeAnna L. Ledford,[c] Ashlee Tietje,[d] Andrew A. Kelso,[c] Michael G. Sehorn,[c] Yanzhang Wei,[d] Mrinmay Chakrabarti,[e] Swapan Ray,[e] and Stephen H. Foulger,*[a,b]

Received Date
Accepted Date

DOI: 10.1039/xxxxxxxxxx

www.rsc.org/journalname

Survivin belongs to the family of inhibitor of apoptosis proteins (IAP) and is present in most cancers while being below detection limits in most terminally differentiated adult tissues, making it an attractive protein to target for diagnostic and, potentially, therapeutic roles. Sub-100 nm poly(propargyl acrylate) (PA) particles were surface modified through the copper-catalyzed azide/alkyne cycloaddition of an azide-terminated survivin ligand derivative (azTM) originally proposed by Abbott Labs and speculated to bind directly to survivin (protein) at its dimer interface. Using affinity pull-down studies, it was determined that the PA/azTM nanoparticles selectively bind survivin and the particles can enhance apoptotic cell death in glioblastomas and other survivin over-expressing cell lines such as A549 and MCF7 relative to cells incubated with the original Abbott-derived small molecule inhibitor.

1 Introduction

A prophetic indicator of cancerous cells is their circumvention of programmed cell death (apoptosis). The maintenance of tumors has been speculated to be achieved through nodal proteins that are involved in multiple signaling mechanisms[1]. One such protein *survivin* (BIRC5), a member of the inhibitors of apoptosis (IAP) family, is vital for cellular homeostasis, playing a role in cell division and cell death[2], This protein is abundant in embryonic and fetal development[3], but is below detection limits in most terminally differentiated adult tissues[4–6], though it has been detected in primitive hematopoietic cells, T lymphocytes, polymorphonuclear neutrophils, and vascular endothelial cells[7]. A number of studies have shown that survivin is overexpressed in human cancers and its appearance in a patient results in an increased risk factor for cancer progression and a poor prognosis[4,8–12]. Survivin appears to bestow on tumor cells an enhanced adaptability, capacity to proliferate, and aversion to cell death[13–15]. Achieving apoptosis is integral to the cytotoxic activity of most chemotherapeutic drugs and radiation therapies and their reduced potency stems from antiapoptotic proteins[16]. In an effort to enhance the potency of cancer therapies, the targeting of antiapoptotic proteins expressed by cancer cells has become an important approach to cancer treatment[17].

The focus on survivin as a means to combat cancer through a mitigation of its antiapoptotic functions has resulted in a number of inhibition or sequestration strategies, with only three inhibitors reaching clinical trials by 2013[18]. These inhibition or sequestering strategies can be divided into four broad categories: (1) molecular antagonists (antisense oligonucleotides, siRNA, and transfection of a plasmid encoding the dominant-negative survivin) based inhibition[19–26]; (2) gene therapy with small molecules such as YM155 or FL118[27–30]; (3) immunotherapy, where the immune cells such as natural killer cells, dendritic cells, and cytotoxic T lymphocytes, are isolated from the patient, activated *in vitro* and transfused back to the patient to target cancer cells[18,31,32]; and (4) survivin binding small molecules which attach to the protein to disrupt its antiapoptotic function[33,34]. The antisense or siRNA approaches may result in undesirable broad phenotypic consequences, effecting normal cells and exhibit varying anti-cancer potency *in vitro*, *in vivo*, and in humans[18,22,35]. There is also a lack of appreciation in how these antisense oligonucleotides distribute to tissues and are taken up by cells in the human body[36]. The dominant-negative survivin method in treating cancers is still clinically impractical, as the mutant protein is unstable in the blood stream[18]. Phase II clini-

† Electronic Supplementary Information (ESI) available: [details of any supplementary information available should be included here]. See DOI: 10.1039/b000000x/

* To whom correspondence should be addressed; E-mail: foulger@clemson.edu.
[a] *Center for Optical Materials Science and Engineering Technologies, Department of Materials Science & Engineering, Clemson University, Clemson, SC 29634, USA.*
[b] *Department of Bioengineering, Clemson University, Clemson, SC 29634, USA.*
[c] *Department of Genetics & Biochemistry, Clemson University, Clemson, SC 29634, USA.*
[d] *Department of Biological Sciences, Clemson University, Clemson, SC 29634, USA.*
[e] *Department of Pathology, Microbiology, & Immunology, University of South Carolina School of Medicine, Columbia, SC 29209, USA.*

cal trials of YM155, a small molecule survivin gene suppressant, failed as adverse effects were reported and the objective tumor response rate (ORR) of patients to the treatment was only 3 - 6 %[37,38]. Immunotherapy is a relatively new strategy compared to the other methods, and investigations are being carried out to find the epitopes that generate the strongest immunodominant, immunoprevalent T-cell reaction against survivin[39]. Finally, the use of small molecule ligand that simply binds to the protein and disrupts survivin's activity may present a more focused and less destructive therapeutic approach if the binding can be designed to only occur in a tumor of interest[30,40]. Unfortunately, the widespread development of new binding ligands for survivin is frustrated by the perceived lack of structural pockets of the appropriate geometry and hydrophilicity on the protein that act as a druggable site[33]. Survivin forms a bow-tie shaped symmetrical homodimer and contains a single baculoviral IAP repeat (BIR) domain, which is common in the IAP family[41]. A newly discovered small molecule binding site at the dimer interface on survivin, which is distinct from the BIR site, has been recently reported[33]. This second potential binding site appears to possess a higher propensity for small-molecule binding than the BIR site, though the functional role of this site is currently unknown. Nonetheless, it is speculated that the interface site may be involved in binding to other proteins that regulate survivin function of inhibiting apoptosis[33,42]. Recently, high-affinity small molecule "survivin ligands" have been proposed by Abbott Laboratories for binding to the site[33] and, based on their structural variability, this site may be a biologically relevant protein binding site that can be targeted with small molecule drugs. The small molecule ligand binds at the dimer interface and frustrates the binding of other proteins to the site, leading to the activation of apoptosis. A recent effort[42] has focused on a modified Abbott ligand[33] that was designed to disrupt the Survivin-Ran protein complex, a complex identified to promote spindle formation in tumor cells[43].

All the strategies mentioned previously exhibit varying degrees of success for disrupting the function of survivin, but all suffer from inherent problems such as systemic toxicity, reduced bioavailability, and ineffective delivery[18]. These setbacks can be overcome by employing different delivery platforms such as liposomes, dendrimers, and polymeric nanocarriers that can enhance a drug's protection, availability, and tissue distribution[18], resulting in an improved effectiveness[18,44–49]. To this end, a small molecule drug that binds to survivin was modified to allow its attachment to the surface of sub-100 nm polymer particles to assess its propensity to bind with survivin and its effectiveness in inducing apoptosis relative to the "free" drug. Specifically, the "survivin ligand" developed by Abbott labs was selected for this comparison[33]. In this current effort, the ligand was modified to include an azide group and attached to poly(propargyl acrylate) nanoparticles through an azide/alkyne Huisgen cycloaddition using a copper catalyst. These surface-modified particles were incubated with various cancer cell lines that are known to overexpress survivin. The extent of survivin sequestration and resulting enhancement in apoptosis was assessed.

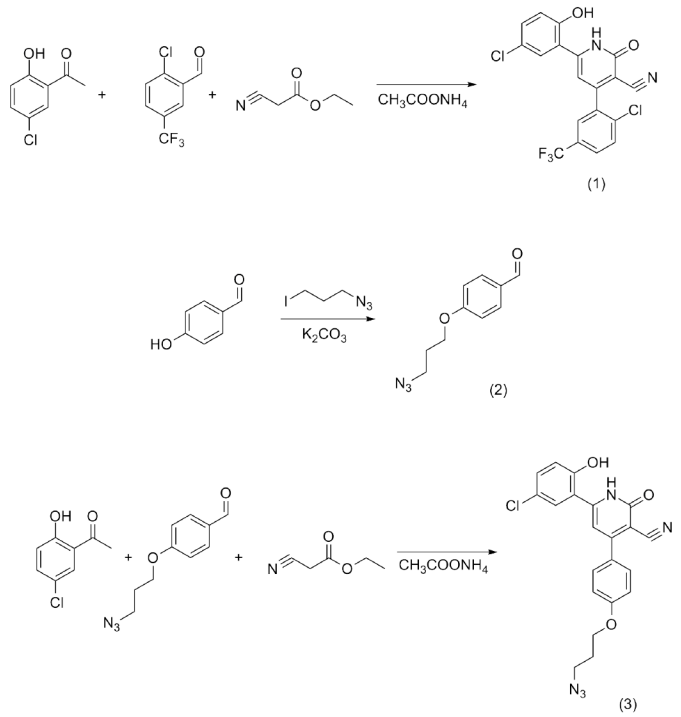

Fig. 1 Reaction scheme for synthesis of survivin ligands, TM and azTM

2 Experimental

2.1 Reagents and solvents.

All the commercial reagents were purchased from TCI America and Alfa Aesar and used without further purification. All the solvents were dried according to standard methods. Deionized water was obtained from a Thermo Scientific Barnstead NANOpure Water Purification System and exhibited a resistivity of ca. 10^{18} $ohm^{-1}cm^{-1}$.

2.2 Chemical characterization methods.

^{1}H and ^{13}C NMR spectra were recorded on JEOL ECX-300 spectrometers (300MHz for proton and 76MHz for carbon). Chemical shifts for protons are reported in parts per million downfield from tetramethylsilane and are referenced to residual protium in the NMR solvent ($CDCl_3$: δ 7.26 ppm, DMSO-d6: δ 2.50 ppm). Chemical shifts for carbons are reported in parts per million downfield from tetramethylsilane and are referenced to the carbon resonances of the solvent ($CDCl_3$: δ 77.16, DMSO-d6: δ 39.52 ppm). Coupling constants are reported in Hertz (Hz). LC/MS mass spectra were obtained using Finnigan LCQ spectrometer and HP 1100 (HPLC). The IR spectra were recorded at room temperature in the wavenumber range of 400-4000 cm^{-1} and referenced against air with a Nicolet 6700 FTIR instrument. A total of 32 scans were averaged for each sample at 2 cm^{-1} resolution.

2.3 Preparation of survivin ligands (TM and azTM)

The survivin ligand TM was prepared based on the method published[33,50,51]. The reaction scheme for the synthesis of TM is presented in Figure 1.

This journal is © The Royal Society of Chemistry [year]

6-(5-chloro-2-hydroxyphenyl)-4-(2-chloro-5-(trifluoromethyl)phenyl)-2-oxo-1,2-dihydropyridine-3-carbonitrile (1) 1-(5-Chloro-2-hydroxyphenyl) ethanone (0.1 g, 0.586 mmol), 2-chloro-5-(trifluoromethyl) benzaldehyde (0.122 g, 0.586 mmol), ethyl cyanoacetate (0.1 g, 0.88 mmol), and ammonium acetate (0.45 g, 5.86 mmol) were dissolved in ethanol (7 mL) and stirred under nitrogen atmosphere in sealed flask at 110 ^{o}C for 3 hours. After cooling, the precipitated yellow solid was diluted with diethyl ether (7ml), filtered, washed with diethyl ether and with water, and then dried to give the product. Yield: 0.1 g (40 %). m.p. = 330 ^{o}C with destruction. ^{1}H NMR (DMSO-d6) δ 6.69 (d, 1H, J = 8.9 Hz), 6.83 (s, 1H), 7.15 (d.d, 1H, J = 8.9 Hz, J= 2.6 Hz), 7.82 (m, 1H), 7.86 (m, 1H), 7.88 (m, 2H); 8.02 (d, 1H, J= 2.6 Hz). ^{13}C NMR (DMSO-d6) δ 95.78, 102.78, 117.52, 118.18, 120.00, 120.60, 121.86, 125.46, 127.10, 127.30 (m), 127.83, 128.26, 130.81, 131.63, 135.75, 137.77, 154.11, 155.33, 161.92, 163.50. ESI-Mass m/z (%): 426.7 (75), 423.27 ([M-H]$^{-}$; 100).

The reaction scheme for the synthesis of azTM is presented in Figure 1.

4-(3-azidopropoxy)benzaldehyde (2) *p*-Hydroxybenzaldehyde (0.1 g, 0.82 mmol) and 1-azido-3-iodo propane (0.19 g, 0.9 mmol) were dissolved in acetone (15 mL). Potassium carbonate (0.113 g, 0.82 mmol) was added to the solution and obtained mixture was stirred and refluxed for 5 hours. After cooling the mixture was quenched with water and extracted with dichloromethane. Organic layer was separated, dried with Na_2SO_4 and filtered. The filtrate was evaporated to give a clear oil. Yield: 0.13 g (77 %). ^{1}H NMR ($CDCl_3$) δ 2.09 (m, 2H, J = 6.3 Hz), 3.54 (t, 2H, J = 6.5 Hz), 4.14 (t, 2H, J = 6.0 Hz), 7.00 (d, 2H, J = 8.6 Hz), 7.80 (d, 2H, J = 8.6 Hz), 9.88 (s, 1H).

4-(4-(3-azidopropoxy)phenyl)-6-(5-chloro-2-hydroxyphenyl)-2-oxo-1,2-dihydropyridine-3-carbonitrile (3) 1-(5-Chloro-2-hydroxyphenyl)ethanone (0.277 g, 1.62 mmol), 4-(3-azidopropoxy)benzaldehyde (0.4 g, 1.95 mmol), ethyl cyanoacetate (0.238 g, 2.11 mmol) and ammonium acetate (0.75 g, 9.72 mmol) were dissolved in ethanol (7 mL) and stirred under nitrogen atmosphere in sealed flask at 110 ^{o}C for 16 hours. After cooling, the precipitated yellow solid was filtered, washed with cold ethanol and with water, and then dried. Obtained yellow solid (0.265 g) is the mix of two compounds with same molecular weight. The mix was separated by flash column chromatography on silica, solvent ethyl acetate : hexane (1 : 1). R_F=0.8. Yield: 0.105 g (15 %). m.p. = 186 ^{o}C with decomposition. ^{1}H NMR (DMSO-d6) δ 2.02 (m, 2H, J = 6.5 Hz), 3.54 (t, 2H, J = 6.5 Hz), 4.13 (t, 2H, J = 6.0 Hz), 7.05 (d, 2H, J = 8.9 Hz), 7.36 (d, 1H, J = 8.9 Hz), 7.60 (d.d, 1H, J = 2.4 Hz, J = 8.9 Hz), 7.92 (s, 1H), 8.28 (d, 2H, J = 8.9 Hz), 8.65 (d, 1H, J = 2.4 Hz). ^{13}C NMR (DMSO-d6) δ 28.16, 47.73, 64.87, 95.28, 100.27, 114.37, 118.72, 119.0, 124.65, 129.05, 129.29, 130.05, 132.0, 143.41, 150.60, 160.18, 160.48, 160.65. ESI-Mass m/z (%): 423 (70) [M+H]$^{+}$, 418 (100).

2.4 Preparation of azide-modified polyethylene glycol (azPEG).

The azPEG was prepared according to the method published[52].

Mono-methoxy-PEG5000-methansulfonate Methylsulfonyl chloride (0.92 g, 8 mmol) in dichloromethane (5 mL) was added dropwise at room temperature to the stirring solution of triethylamine (0.89 g, 8.8 mmol) and mono-methoxy-PEG5000 (20 g, 4 mmol) in dichloromethane (70 mL). The solution was stirred at 20 ^{o}C for 4 hours, then washed with water and the organic layer was dried with Na_2SO_4 with further filtration. The solvent was evaporated under vacuum to give the product as a white solid. Yield: 20.3 g (97 %). ^{1}H NMR ($CDCl_3$) δ 3.07 (s, 3H), 3.36 (s, 3H), 3.48 (t, 2H), 3.53 (m, 2H), 3.62 (m, ca. 400H), 3.75 (m, 4H), 4.36 (m, 2H).

Mono-methoxy-PEG5000-azide The mixture of mono-methoxy-PEG5000-methansulfonate (20.3 g, 4 mmol) and sodium azide (1.1 g, 17 mmol) in acetonitrile (80 mL) was refluxed and stirred for 15 hours. After cooling, the mixture was filtered and the solvent was evaporated. The residue was dissolved in dichloromethane and washed with water, organic layer was separated, dried with Na_2SO_4 and filtered. The solvent was evaporated, the crystalline residue was washed with hexane, filtered and dried in air to give the product as a white solid. Yield: 19 g (94 %). ^{1}H NMR ($CDCl_3$) δ 3.35 (s, 3H), 3.38 (t, 2H), 3.62 (m, ca. 400H), 3.85 (m, 2H). FTIR (cm^{-1}): 1095 (s, C-O-C); 1340, 1465 (CH2); 2100 (N3); 2880 (s, CH2).

2.5 Preparation of the particles.

Propargyl acrylate (PA) particles were prepared according to a standard emulsion polymerization method published[52].

For a typical surface modification of the particles, for example, the grafting of azTM and azide-modified PEG chains with molecular weight of 5000 (azPEG) onto the particles, 1 mL PA particles and 5 mg azTM were added to 2 mL of deionized water. Solutions of 0.07624 g copper(II) sulfate (99.999% Aldrich) in 10 mL deionized water and 0.3024 g sodium ascorbate (99% Aldrich) in 10 mL deionized water were made. Initially, 0.5 mL of the $CuSO_4$ solution was added to the PA/ azTM solution, followed by 0.5 mL of the sodium ascorbate solution. The resulting mixture was maintained at a temperature of ca. 28 ^{o}C for 15 minutes and then the reaction was stopped by the removal of unreacted azTM, sodium ascorbate, and Cu(II)SO_4 through a repeated particle washing procedure consisting of centrifugation and redispersement in methanol. The cleaned PA/ azTM particles in water were subsequently utilized in a secondary click transformation with 54.99 mg azPEG, and previously presented $CuSO_4$ and sodium ascorbate solutions. The reaction was allowed to run for 24 hours and then washed to remove unreacted species as determined by absorbance measurements; these particles are referred to as PA/ azTM/ azPEG particles.

2.6 Calculation of grafting densities

The molar extinction coefficient of the free ligand in the dilute regime and wavelength range of 370 nm to 410 nm is used to estimate the number of fluorophores attached to the particles.

First, the molar extinction coefficient for the survivin ligand in the dilute regime is measured. The concentration of the modified particles solution is estimated using Beer's law (A = εbc where A is absorbance, ε is molar extinction coefficient, in $M^{-1}cm^{-1}$, b is path length in cm, and c is concentration in M). 500 μL of the modified particles solution is dried out to measure the mass. The diameter of the unmodified particle is measured using the DLS (Dynamic Light Scattering) and the surface area, mass and volume of a particle are calculated. Using the mass of a particle and the mass of 500 μL of solution, the number of modified particles per mL is calculated by assuming that the mass of the dye is negligible compared to the mass of the particle. Finally, the concentration and number of particles is used to determine the grafting density and distance between two chromophores.

2.7 Affinity pull-down assay.

The particles (conjugated or control) were washed 3 times with Buffer A (20 mM KH_2PO_4 pH 7.5, 10 % glycerol, 0.5 mM EDTA, 0.01 % Igepal, and 1 % Triton) before the addition of survivin-$HIS_{(6)}$ or BSA (6 μg each). The reactions were agitated at 4 ^{o}C for 30 min in Buffer B containing 150 mM KCl (final volume of 30 μL). The supernatant was removed from the beads followed by 3 washes of the beads with Buffer A containing 300 mM KCl. Equal volumes of 2x SDS dye was added to the supernatant and wash fractions, while 30 μL of 2xSDS loading dye was added to the bead fraction. The fractions were subjected to SDS-PAGE analysis on 15 % gels followed by Coomassie Blue staining.

2.8 Cell analysis.

Human A549, MCF7, and U118MG cell lines were obtained from ATCC (Rockville, MD). Human glioblastoma U251MG cell line was obtained from National Cancer Institute (Frederick, MD). A549 cells were cultured in F-12K media (Kaighn's Modification of Ham's F-12 medium) containing 10 % fetal bovine serum (FBS) and 1 % antibiotic. MCF7 cells were cultured in phenol red-free Dulbecco's modified Eagle's media (DMEM) containing 10 % fetal bovine serum (FBS) and 1 % Penicillin-Streptomycin. U118MG cells were cultured in Dulbecco's modified Eagle's media (DMEM) containing 10 % fetal bovine serum (FBS) and antibiotics. U251MG cells were cultured in Roswell Park Memorial Institute (RPMI) 1640 containing 10 % fetal bovine serum (FBS) and antibiotics. Cells were cultured at 37 °C in a humidified atmosphere of 95 % air 5 % CO_2.

2.9 Cytotoxicity assay.

A549 cells (5,000 cells per well) were cultured on 96 well plates for 24 hours. Subsequently, cells were, exposed to 15 and 20 μM of PA, 15 and 20 μM of PA/ azPEG, 1, 6.5, 25, 45, and 65 μM of azTM, 1, 6.5, 25, 45, and 65 μM of PA/ azTM and 1, 6.5, 25, 45, and 65 μM of PA/ azTM/ azPEG. After 48 hours, cell death was assessed with a MTS assay according to the manufacturer's instructions (Promega, Madison, WI). Briefly, medium was aspirated and a solution of 100 μL of F-12K containing 10% FBS and 3-(4,5-dimethylthiazol-2-yl)-5-(3-carboxymethoxyphenyl)-2-(4-sulfophenyl)-2H-tetrazolium, salt (MTS) and phenazine methosulfate (PMS) was added onto each well. After 150 minutes, wells were scanned colorimetrically at 490 nm on a spectrophotometer. The conversion of MTS into an aqueous soluble formazan product is achieved only by dehydrogenase enzymes, which are present in metabolically active cells; the absorbance at 490 nm from the formazan product is directly proportional to the number of living cells in culture. MCF7 cells (20,000 cells per well) were cultured on 96 well plates for 24 hours. Subsequently, cells were, exposed to 1, 6.5, 25, 45, and 65 μM of azTM, 1, 6.5, 25, 45, and 65 μM of PA/ azTM and 6.5, 25, 45, and 65 μM of PA/ azTM/ azPEG. After 72 hours, cell death was assessed with a MTS assay according to the manufacturer's instructions (Promega, Madison, WI). Briefly, medium was aspirated and a solution of 100 μL of DMEM containing 10% FBS and 3-(4,5-dimethylthiazol-2-yl)-5-(3-carboxymethoxyphenyl)-2-(4-sulfophenyl)-2H-tetrazolium, salt (MTS) and phenazine methosulfate (PMS) was added onto each well. After 180 minutes, wells were scanned colorimetrically at 490 nm on a spectrophotometer. Human glioblastoma U118MG and U251MG cells were cultured on 96 well plates for 24 hours. Subsequently, cells were, exposed to 0.05, 0.1, 0.25, 0.5, 1.0, and 2.5 μM of TM and 0.05, 0.1, 0.25, 0.5, 1.0, and 2.5 μM of azTM. The growth medium was supplemented with 2 % FBS and treated with TM or azTM. After 24 hours, cell death was assessed with a MTT assay according to the manufacturer's instructions. Briefly, medium was aspirated and a solution of DMEM containing 10 % FBS and 0.2 mg/ mL MTT was added onto each well. After 180 minutes, DMSO (200 μL) was added to each well to dissolve the formazan crystals and absorbance was measured at 570 nm with background subtraction at 630 nm. Cell viability was presented as percentage of viable cells in total population. Significant difference from control value was indicated by $^*p < 0.05$.

2.10 In situ Wright staining for the detection of morphological features of apoptosis.

The U118MG and U251MG cells were grown in 6 - well plates and treated with TM (0.1, 0.5, or 1.0 μM) or azTM (0.1, 0.5, or 1.0 μM) for 24 hours. At the end of treatments, both adherent and floating cells were centrifuged at a low rpm to sediment them. The cells were then washed twice with PBS, pH 7.4, before being fixed and subjected to in situ Wright staining. The 6 - well plates were then allowed to dry and cells (n = 300) were examined under the light microscope. The morphology of the apoptotic cells as examined under light microscopy included such characteristic features as chromatin condensation, cell-volume shrinkage, and membrane-bound apoptotic bodies. Four randomly selected fields were counted for at least 300 cells. The percentage of apoptotic cells was calculated from three separate experiments.

2.11 Western blotting using specific antibodies.

Both glioblastoma cell lines (U118MG and U251MG) were treated with azTM or PA/ azTM (1.0 μM survivin ligand concentration) prior to extraction of protein samples. The protein samples (10 μg) were mixed with Laemmli composition of buffer and boiled in water for 5 min. The boiled protein samples were loaded

This journal is © The Royal Society of Chemistry [year]

onto precast 4 - 20 % polyacrylamide gradient gels (Bio-Rad Laboratories, Hercules, CA) and electroblotted to the polyvinylidene fluoride (PVDF) membranes (Millipore, Bedford, MA). The non-specific binding sites in the membrane were blocked with 5 % non-fat dry milk for 1 hour at room temperature. The membranes were then incubated overnight at 4 ^{o}C on a rocker with appropriate dilution of primary IgG antibody followed by three times washing in washing buffer (20 mM Tris-HCl, pH 7.6, 137 mM NaCl, 0.1 % Tween 20). After washing, the membranes were incubated with the appropriate alkaline horseradish peroxidase (HRP)-conjugated secondary IgG antibody for 1 hour followed by three times washing in washing buffer. Specific protein bands were detected by incubation for 5 min at room temperature with Immun-StarTM HRP Lumino/Enhancer (Bio-Rad Laboratories, Hercules, CA) and exposing to BIOMAX XAR films (Kodak, Rochester, NY) for autoradiography. The antibody against β-Actin (clone AC-15) was purchased from Sigma (St. Louis, MO), and antibodies against survivin and caspase-3, were from Santa Cruz Biotechnology (Santa Cruz, CA). The alkaline HRP-conjugated anti-rabbit and anti-mouse secondary IgG antibodies were purchased from Biomeda (Foster City, CA) and anti-goat secondary IgG antibody was from Santa Cruz Biotechnology (Santa Cruz, CA). The autoradiograms were scanned on an EPSON Scanner using Photoshop software (Adobe Systems, Seattle, WA, USA) and optical density (OD) of each band was determined using the NIH Image software. The OD of bands in the control treatment was designated as 100. All experiments were performed in triplicates and results were analyzed for statistical significance.

2.12 Determination of apoptotic,necrotic and healthy cells

A549 cells (5,000 cells per well) were cultured on 96 well plates for 24 hours. Subsequently, cells were exposed to 25 μM of azTM, unmodified PA particles, PA/ azTM particles of two different grafting densities of 0.63 and 1.77 azTM/ nm^2, and PA/ azTM/ azPEG particles. After 24 hours of treatment, the apoptotic, necrotic and healthy cells quantification kit purchased from Biotium, Inc. (Hayward, CA, USA) was used according to the manufacturer's instruction. The stained cells were observed under a Life Technologies EVOS® FL Cell Imaging System using filter sets of DAPI, GFP and RFP. Healthy cells were stained with Hoechst 33342 and had only blue emission. Necrotic cells were stained with Hoechst 33342 and Ethidium homodimer III, and had both blue and red emissions. Apoptotic cells had blue, red and green emissions as those cells were stained by all the three stains: Hoechst 33342, Ethidium homodimer III and fluorescein labeled Annexin-V. Cells stained by the triple colors indicate dead cells progressing from apoptotic cell population[53,54]. All the three types of cells were counted and expressed as percentage of total cells.

3 Results & Discussion

Figure 2 presents the structures of the survivin-binding ligands and the proposed route for "capturing" free survivin with nanoparticles surface modified with ligands. As indicated earlier, prior art has focused on several survivin inhibition approaches, such as, antisense oligonucleotides targeting mRNA,

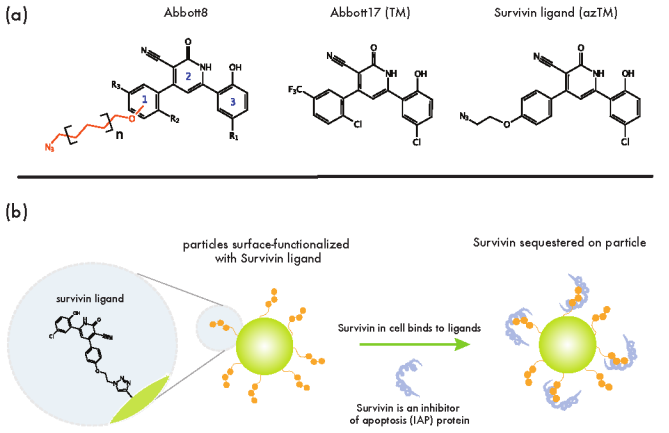

Fig. 2 **(a)** Structures of survivin ligands, Abbott8 and Abbott17 (targeting molecule TM) proposed by Abbott Labs and an azide modified targeting molecule (azTM). **(b)** Schematic of poly(propargyl acrylate) (PA) particles surface modified with an azide-terminated survivin ligand (azTM) through an aqueous-phase "click" transformation sequestering anti-apoptotic protein survivin.

immunotherapeutic strategies, and small molecule binding to the BIR (Baculoviral IAP repeat) domain. A new binding site at the dimer interface of survivin, distinct from the BIR site, has been recently identified and appears to have an increased binding to small molecules and may be useful for targeting & inhibition. Recently, high-affinity small molecule "survivin ligands" have been proposed for binding to the site by Abbott Labs with binding constants (K_D) ranging from 0.037 μM to 0.88 μM and were obtained by monitoring the chemical shift changes as a function of ligand concentration[33]. According to their studies, a favorable binding of a small molecule to the dimer interface is indicated by a small value binding dissociation constant, K_D. A K_D value of sub-5 μM suggests a relatively strong affinity. In their studies, it was speculated that the dimer interface plays an important role in binding to other proteins which serve a role in apoptosis. This was subsequently proven with a variant of an Abbott Labs compound (4-(3,5-Bis(benzyloxy)phenyl)-6-(5-chloro-2-hydroxyphenyl)-2-oxo-1,2-dihydropyridine-3-carbonitrile; LLP3) which also binds to the dimer interface of survivin and was utilized to prevent Ran from binding to survivin and forming a Survivin-Ran protein complex. This disruption allowed the native apoptosis pathway to continue[43].

Figure 2a presents the Abbott8 compound (with labeled rings) employed by Abbott to establish the structure-activity relationship (SAR) of the survivin ligand. In these original studies, ligands that bind to survivin shared in a number of structural characteristics. Through high temperature superconductor (HTS) NMR studies[33], it was determined that Ring-2 must be a central pyridone, while Ring-3 must be a phenol, so that a hydrogen bonding network can form, via the 2-hydroxypyridine central ring tautomer, forcing the two rings into a coplanar arrangement. In addition, a cyano group must be on the center ring (Ring-2)[33,55] for binding, though NMR structures provided no indication of a specific interaction with survivin. Replacing this latter group with carboxamide, methyl, halogen, or hydrogen all greatly diminished

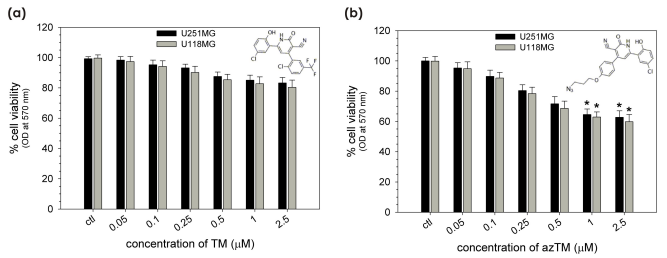

Fig. 3 Preliminary cell viability data in glioblastoma cells, U251MG and U118MG, using MTT assay. Untreated cells were used as the control (ctl). Cells were treated with the small molecule ligands at the indicated concentrations for 24 hours. Cell viability is presented as a percentage of viable cells in the total population. Significant difference from control value was indicated by *p<0.05. **(a)** TM and **(b)** azTM treatment of the glioblastomas.

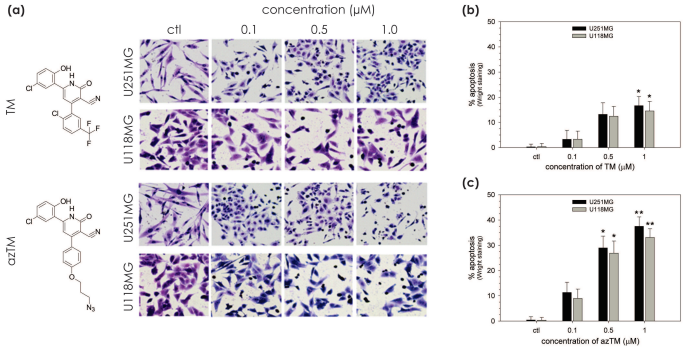

Fig. 4 Increased apoptosis in glioblastoma cells, U251MG and U118MG, with azTM small molecule ligand when compared to TM. Untreated cells were used as the control (ctl). Cells were treated with TM or azTM ligand at indicated concentrations for 24 hours. **(a)** In situ Wright staining for detection of morphological features of apoptosis. Bar diagram shows percent apoptosis based on Wright staining for **(b)** TM and **(c)** azTM treatments. Cell death is presented as percentage of apoptosis in total population. Significant difference from control value was indicated by *p < 0.05 or **p < 0.01.

binding[33]. In addition, only hydrophobic groups were preferred when substituted into Ring-1. On this latter ring, substitutions on 2,4 and, particularly, 2,5 with chlorine and methyl groups at the 2 position, with chlorine, methyl, and CF_3 substitution at the 4 and 5 positions resulted in energetically acceptable structures[33]. In the current effort, azide terminated methoxyalkanes with $(CH_2)_n$ of n=2 at position 4 of Ring-1 (Figure 2a; azTM) was employed to covalently attach the ligand to a poly(propargyl acrylate) (PA) particle through a copper-catalyzed click transformation (cf. Figure 2b).

3.1 *in vitro* viability and apoptosis studies of survivin ligands in glioblastomas.

Currently, there are not many *in vitro* cytotoxicity studies in the literature that demonstrate that the Abbott-derived survivin ligands can disrupt survivin activity and induce apoptosis[40,42,56,57]. To that end, the survivin ligand originally proposed by Abbott Labs (6-(5-Chloro-2-hydroxyphenyl)-4-[2-chloro-5-(trifluoromethyl)phenyl]-2-oxo-1H-pyridine-3-carbonitrile; TM) and its structural analog modified with an azide linker (4-[m-(2-Azidoethoxy) phenyl]-6-(5-chloro-2-hydroxyphenyl)-2-oxo-1H-pyridine-3-carbonitrile; azTM) (cf. Figure 2a) were synthesized and tested to verify their potential for survivin activity disruption in two human glioblastoma cell lines, specifically U251MG and U118MG, which exhibit survivin overexpression[8]. Glioblastomas are the most common form of malignant primary brain tumors and they have a propensity to encroach quickly into the surrounding tissues, frustrating surgical routes to their removal[8,15]. These tumors were chosen for study as they exhibit an increased resistance to apoptosis and are relatively resistant to radiation and chemotherapy[8,15].

Figure 3 presents the determination of cell viability of targeting molecules, TM or azTM, using the 3-(4, 5-dimethylthiazol-2-yl)-2, 5-diphenyl tetrazolium bromide (MTT) assay. Cell viability is presented as a percentage of viable cells in the total population and a significant difference from the control value was indicated by a p-level with $^*p<0.05$[8,58]. The original Abbott-developed drug TM exhibited a ca. 10% reduction in cell viability for both cell lines that was not statistically significant, while the azide-modified version azTM resulted in a statistically significant reduction of ca. 30 % in viability for both cell lines at a dosage of 2.5 μM. A cell death of over 30 % at a dosage of 2.5 μM indicates a high ratio in comparison to other survivin activity disruption studies; a study on the cytotoxicity in glioblastomas of a number of small molecules derived from 6-(*o*-Hydroxyphenyl)-2-oxo-4-phenyl-1H-pyridine-3-carbonitrile (i.e. Abbott8)[33] was recently presented[42]. In this study, the IC_{50} value for the lead compound (LLP3), a variant of Abbott8, was determined to be 31.2 μM, which is an order of magnitude greater than that of azTM for a similar efficacy. Assuming that the enhancement is due to an increased survivin binding to azTM, the structural difference between TM and azTM is localized to Ring-1 (cf. Figure 2). The substitution of the trifluoromethyl group and chlorine on Ring-1 with the azidoethoxy group is speculated to enhance the binding of the drug to the dimer interface of survivin[33]. The occupancy of the dimer interface has been theorized to interfere with survivin's binding to other proteins which are required to activate its IAP functions. Specifically, LLP-3 was designed from Abbott8, the targeting molecule used in this project, by adding 2 phenyl rings to displace the Leu98 and Leu102 interactions in survivin dimerization and weaken the protein-protein interface and results in blocking the binding of survivin to Ran[42,59]. GTP-binding nuclear protein Ran is a protein that is encoded by the RAN gene in humans and is a regulator of bipolar mitotic spindle assembly.

The observed efficacy of azTM in promoting cellular death in the U251MG and U118MG cell lines could be through an enhanced apoptosis (desired programmed cell death) or simply toxicity of the drug. In order to identify apoptotic cells, a standard *in situ* Wright staining study was employed (cf. Figure 4a)[60–65]. Typical morphologic changes in cells undergoing apoptosis include cell shrinkage, enhanced round shape, chromatin condensation, blebbing of cell membrane, and enhanced refractivity of cells under phase-contrast imaging[66]. Utilizing these visual de-

This journal is © The Royal Society of Chemistry [year]

scriptors, the cells treated with TM and azTM at a concentration of 0.1, 0.5, and 1.0 μM were compared to the untreated control cells and observed the morphological features of apoptotic cells (cf. Figure 4). Figure 4b presents the number of cells undergoing apoptosis relative to the control, and while both drugs resulted in enhanced apoptosis in both cells lines, azTM resulted in a greater proportion of cells exhibiting these feature at a set concentration relative to cells incubated with TM. The azTM treatment with 1 μM induced more than 35 % apoptosis in both cell lines and corresponds to the cell death observed in the viability study (cf. Figure 3). This data is presented in a bar graph in Figure 4b. These results confirm that azTM induces apoptosis and disrupts survivin activity more effectively than the original TM small molecule ligand.

3.2 Surface-functionalized particles.

The previous studies are promising and indicate that the Abbott derived Survivin targeting ligands are a potential tool for survivin activity disruption as a small molecule. However, small molecules have a short *in vivo* circulation lifetime, which limits the feasibility of survivin ligands for use in therapies. To circumvent this issue, the small molecule azTM can be attached to poly(propargyl acrylate) (PA) nanoparticles to increase circulation times and at the same time allowing the ligands to form beneficial host/ guest assemblies. A schematic of the particles studied in this effort is presented in Figure 2b. The PA colloids were prepared using a standard aqueous emulsion polymerization technique resulting in spheres with a diameter of 66.1 $\pm$ 0.26 nm (average and standard deviation). To functionalize the surface of the particles, a multiple step copper-catalyzed azide/alkyne cycloaddition ("click" transformation) was performed in water to produce PA particles that had survivin ligand and polyethylene glycol (PEG) attached to their surface. We have demonstrated previously that these modified particles are free of all the copper used and these cleaned particles are not toxic to cells[52,67]. In addition cytotoxicity tests were carried out using PA/ azPEG particles (cf. Figure 7) to verify that these particles are not toxic. The use of PEG to infer a hydrophilicity to the particles has been found to be important for directing protein absorption in the particles and achieving long circulation times[68].

3.3 Selective binding of functionalized particles.

As stated earlier, prior art suggests that the ligand directly binds at the dimer interface of survivin. Computational modeling of the molecular interactions along the dimerization interface[33,59], affinity screening studies[33], cytotoxicity studies[42,56,57] and fluorescence binding studies of several modified analogs of TM with the wild-type protein and the mutant form of survivin$^{F101A/L102A}$ [42], have been explored to establish the direct binding between the small molecule "free" ligand and survivin, but no studies have been performed to establish the efficacy of the ligands when attached to the surface of nanoparticles. To this end, affinity pull-down experiments were employed. A purification protocol that utilized both affinity and conventional chromatography to purify survivin to near homogeneity was developed (Figure 5a). About 0.4 mg of survivin was obtained from 60 g of bacterial cell pellet. The particles were surface modified with an azide-terminated (azTM) conjugate and poly(ethylene glycol) (azPEG) chains of 5k molecular weight attached to their surface while control particles only had the azPEG modification. After incubation of the particles with purified survivin, the supernatant was removed and the particles were washed with buffer. Any survivin retained on the particles was eluted and subjected to SDS-PAGE analysis. As indicated in Figure 5b, survivin bound the functionalized particles evidenced by its presence in the elution (cf. Figure 5b, lane 4). The interaction with the azTM conjugate is specific since survivin is only present in the supernatant with the control azPEG particles (cf. Figure 5b, lane 10). As expected, bovine serum albumin (BSA) failed to interact with either the azTM or the azPEG.

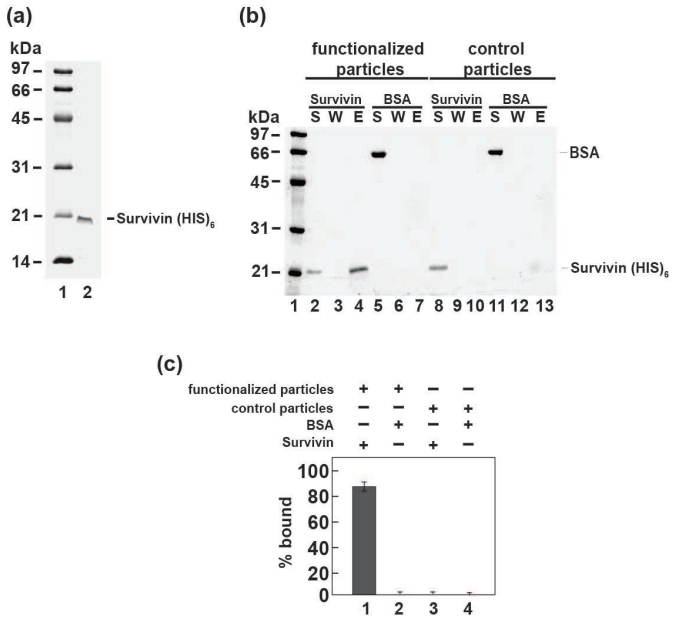

Fig. 5 Purification of survivin and affinity pull-down of survivin by surface-functionalized particles. **(a)** SDS-PAGE of purified recombinant survivin (ca. 0.8 μg); **(b)** Poly(propargyl acrylate) (PA) particles were surface modified with azTM (cf. Figure 2) and azPEG. Control particles lacked the presence of ligand. Both sets of particles were incubated with survivin or BSA protein. The supernatant was removed and the particles were washed with buffer. Proteins retained on the particles were eluted. The supernatant (S), wash (W) and elution (E) were separated on a 15 % polyacrylamide gel and stained with Coomassie blue. **(c)** Percentage of bound proteins on functionalized and control particles (data taken from SDS-PAGE in Part **(b)** as well as two other pull-down experiments).

Figure 5c quantifies the results presented in Figure 5b, as well as two other pull-down experiments. In this figure, the columns of + or - above the graph indicate what combination of particle and protein was employed. For example, in lane 1, the amount of bound survivin on the functionalized particles was quantified while in lane 2, the amount of BSA on the functionalized particles was assessed. Lane 3 & 4 are the control lanes and present the amount of bound protein with survivin & control particles (lane 3) and BSA & control particles (lane 4). These results suggest that

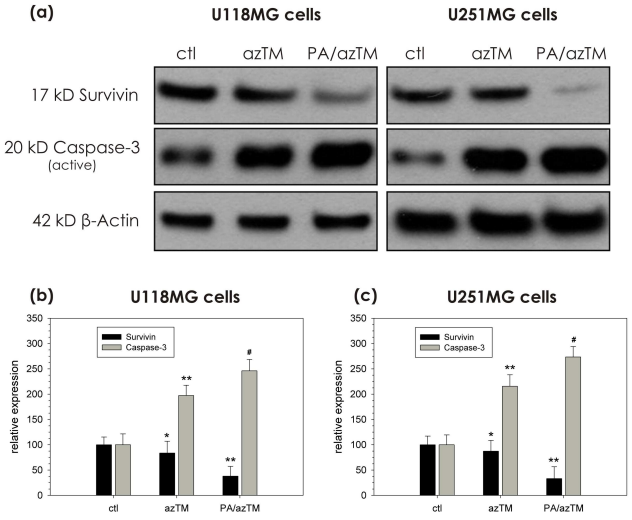

Fig. 6 **(a)** Survivin conjugate azTM disrupted the activity of survivin to promote Caspase mediated apoptosis. Both glioblastoma cell lines were treated with survivin conjugate azTM as a free small molecule or attached to the surface of nanoparticles (1.0 μM ligand concentration) prior to extraction of protein samples. Protein samples were resolved by 4 - 20 % SDS-PAGE and Western blotting was performed using the primary IgG antibodies against survivin, caspase-3, and β-actin. Quantification of expression of survivin and caspase-3 after treatment with free ligand (azTM) and modified particles (PA/ azTM) in **(b)** U251MG or **(c)** U118MG cells. Significant difference from control value was indicated by *p$<$0.1, **p$<$0.01 and #p$<$0.001.

the binding specificity of the survivin ligand is not altered when attached to particles and over 85 % of the survivin bound to the functionalized particles.

3.4 Enhanced apoptosis with functionalized particles.

It's clear that the functionalized particles are capable of selectively binding survivin, but the question remains, will this binding of the protein result in any enhancement of apoptosis of cancer cells. The precise mechanism by which survivin suppresses apoptosis is still in debate, but it is speculated that survivin directly suppresses caspase-3, a protein which is believed to play a central role in the execution-phase of cell apoptosis[14]. To this end, Western blotting for survivin and other proteins involved in Caspase-mediated apoptosis was employed to determine how effectively the modified particles restrain survivin activity in comparison to the "free" drug. Both glioblastoma cell lines were treated with azTM or PA/ azTM nanoparticles (1.0 μM ligand concentration) prior to extraction of protein samples. Protein samples were separated by SDS-PAGE and Western blotting was performed using the primary IgG antibodies against survivin, caspase-3, and β-actin. The horseradish peroxidase conjugated anti-rabbit IgG was used as secondary antibody. Western blots were incubated with ECL detection reagents, exposed to X-OMAT AR films, and photographed (cf. Figure 6). The Western blot indicated that both azTM and PA/ azTM nanoparticles increased the activation of caspase-3, the final executioner of apoptosis, in these glioblastoma cell lines. Importantly, PA/ azTM nanoparticles exhibited a pronounced survivin sequestration relative to the "free" azTM for activation of caspase-3 for apoptosis in both glioblastoma cell lines. Figure 6 presents the quantification of the Western blot data. For both the cell lines, the quantification demonstrated that the caspase-3 expression was increased by 95 % and 140 % for azTM and PA/ azTM, respectively, when compared to the untreated control cells. In addition, it was noticed that for the PA/ azTM treatment, the expression of survivin was decreased by 60 %. This decrease might not be an actual reduction in expression of survivin as it is speculated that the sequestered survivin could have still been bound to the nanoparticles and couldn't be extracted completely for SDS-PAGE and Western blotting studies.

3.5 Viability studies in other cell lines.

To further support and validate the results obtained in the glioblastoma cells, cell viability studies were carried out in the A549 line, cell line known to overexpress survivin[69]. According to National Cancer Institute's anticancer drug screening program, expression of survivin is 20 ng out of 50 μg total protein in A549 cells. Figure 7 presents the cell viability data with A549 cells using the MTS assay. A549 cells are a human alveolar adenocarcinoma cell line which can synthesize lecithin with a high percentage of disaturated fatty acids and are believed to be responsible for pulmonary surfactant synthesis[70]. The cells were treated with azTM and PA/ azTM with two different grafting densities (gd), 0.58 and 1.91 azTM/nm^2, at varying concentrations for 48 hours. In A549 cells, the small molecule and modified particles exhibited the same behavior as exhibited in the glioblastomas cells, though there was an observed dependence on cell reduction with the particle's azTM grafting density. In this A549 line, the "free" molecule exhibited an IC_{50} of 25 μM, while particles with a grafting density of 0.58 gave an IC_{50} between 1 and 6.5 μM. Surprisingly, particles with a higher grafting density of 1.91 gave an IC_{50} that was greater than 25 μM. Similarly, PA/ azTM particles with a low grafting density of 0.77 azTM/nm^2 gave an IC_{50} between 6.5 and 25 μM in MCF7 cells, a human breast adenocarcinoma cell line. Clearly, the dosage of the small molecule azTM when attached to the particles is a combination of particles administered and the grafting density of the ligand to the particle, so a range of particles with grafting densities were investigated. Figure 8 presents the A549 cell viability with particles of varying grafting densities. As a reference point, 1 μM concentration the free ligand (azTM) indicated cell death of ca. 15%, which is lower than the 35 % obtained from glioblastomas (cf. Figure 7). For the "free" molecule, this lower efficiency in the A549 cell line could be due to the fact that the over-expression of survivin in A549 might be higher than in Glioblastomas; it is commonly observed that the efficiency of drugs or targeting molecules varies with different cell lines due to the differing expression levels[69]. From Figure 8, particles with the lowest grafting density (e.g., 0.58 azTM/nm^2) exhibited the greatest impact in cell viability with a 60 % reduction at an azTM concentration of 6.5 μM. Subsequent increases in dosage with the 0.58 azTM/nm^2 particles result in a reduction in efficacy that converge on the cell viability exhibited with particles of higher grafting density. Particles with grafting densities between 0.90

This journal is © The Royal Society of Chemistry [year]

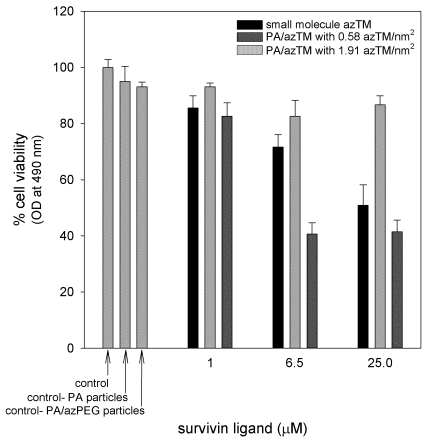

Fig. 7 Cell viability (MTS assay) of A549 cells treated with small molecule azTM and PA/ azTM particles with two different grafting densities (gd), 0.58 and 1.91 azTM/nm^2, at varying concentrations for 48 hours. Unmodified and azPEG modified particles were used as additional controls. Cell viability is presented as percentage of viable cells compared to the control.

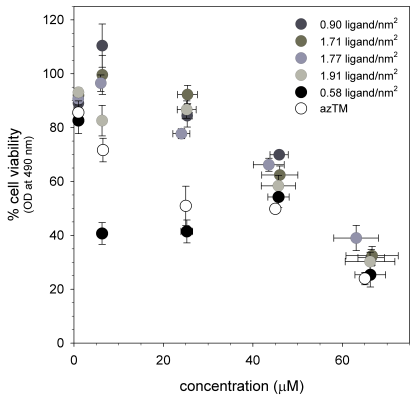

Fig. 8 Viability of A549 cells with PA/ azTM particles of varying ligand surface density. The cells were treated with azTM and PA/ azTM of varying different grafting densities (gd) of 0.58, 0.90, 1.71, 1.77 and 1.91 azTM/ nm^2 and at varying concentrations for 48 hours. Cell viability is presented as percentage of viable cells compared to the control and the MTS assay was employed.

and 1.91 azTM/nm^2 exhibited similar efficacies with a IC_{50} which is greater than 25 μM.

It is speculated that the enhanced IC_{50} values for particles with higher grafting densities was due to an inability of the protein to bind to the particles because of steric concerns. The surface grafting density of 1.91 azTM groups/nm^2 corresponds to a 91 % coverage (on a 67 nm diameter particle) if the distance of an azTM at its widest point (ca. 7.8 Å) can be assumed to define the diameter of a cylinder enclosing the moiety and attached to the PA surface; each particle would then have ca. 29.5k azTM moieties. Similarly, it was noticed that particles modified with both azTM and long azPEG chain (5k) exhibited a decreased percentage of cell death (data not presented). This decrease could be due to the fact that the long PEG chains physically hinder the binding of the ligand with a survivin protein or that a higher dosage is required because the transport of the particles into the cells is reduced with the large hydration shell when the PEGs are attached to the particles [71–74].

3.6 Functionalized particles localized in cells.

Survivin has been found to only operate within the cell. To verify that these particles are taken up by the cells and not just located on the surface of cell, the cells were treated with survivin ligand (azTM) modified particles that are labeled with a near infrared fluorophore squaraine (azSQ), and imaged after 24 hours of incubation. A549 cells were treated with 15 μM PA/ azTM/ azSQ for 24 hours and washed with PBS before imaging. The fluorescence from the squaraine dye was used to identify that the particles were taken up by the cells (cf. Figure 9). In methanol, azSQ has a peak absorption maximum at 663 nm, while the corresponding emission peak is at 672 nm, for a relatively small Stokes shift of 9 nm. This emission of the azSQ labeled particles in Figure 9 clearly show that the modified particles are uptaken by the cells. Due to the low quantum yield of the azSQ, the brightness and contrast

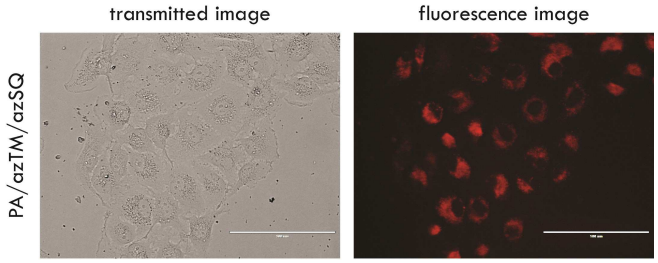

Fig. 9 Imaging of A549 cells treated with 15 μM PA/ azTM/ azSQ for 24 hours and fluorescence images were taken under RFP filter. All scale bars represent 100 μm.

of the image obtained was increased to enhance the emission of the PA/ azTM/ azSQ particles.

In addition, an apoptotic/necrotic/healthy cells detection kit that contains three stains: Hoechst 33342, Annexin V labeled fluorescein, and Ethidium homodimer III, was employed to establish the state of the A549 cells when incubated with PA/ azTM particles. Hoechst 33342 (λ_{abs}/ λ_{em} = 350/461 nm), Annexin V labeled fluorescein (FITC - Annexin V) (λ_{abs}/ λ_{em} = 492/514 nm) and Ethidium homodimer III (EthD-III) (λ_{abs}/ λ_{em} = 528/617 nm) dyes stain healthy, apoptotic and necrotic cells, respectively [75–83]. In the current study, A549 cells were treated for 24 hours with 25 μM of azTM, unmodified PA particles, PA/ azTM particles of two different grafting densities of 0.63 and 1.77 azTM/ nm^2, and PA/ azTM/ azPEG particles. This study is aimed at understanding the qualitative changes in cells with the treatment of azTM and modified particles. To obtain accurate quantitative information a flow cytommetry study can be conducted in future. After the treatment, the cells were stained with the Hoechst 33342, FITC-Annexin V, and EthD-III stains as per the manufacturer's instructions and imaged with a standard fluorescence microscope and Figure 10 presents the images obtained. As expected, for the two control treatments (cf. Figure 10 - panels 1

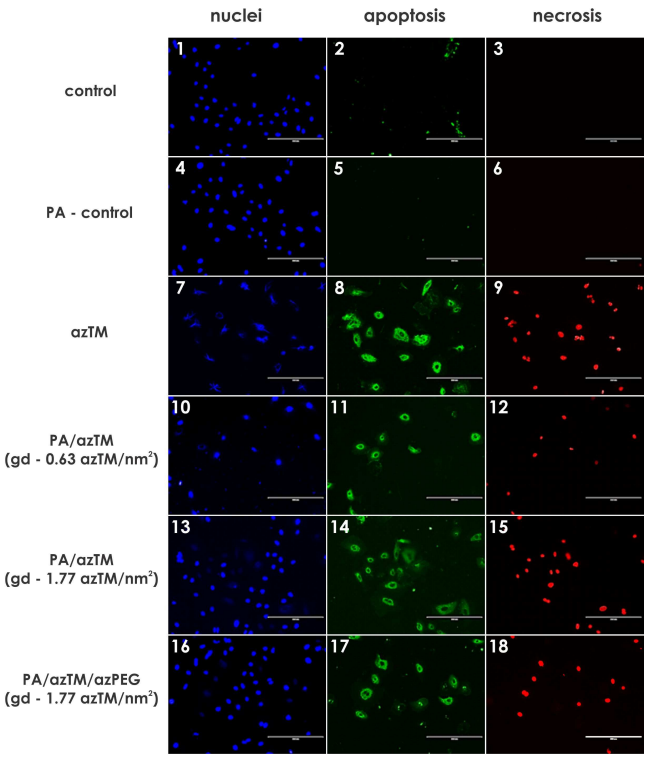

Fig. 10 Fluorescence microscope images of A549 cells after incubation with 25 μM of azTM, PA/ azTM particles with two different grafting densities, PA/ azTM/ azPEG particles and PA particles. Cells were treated with an apoptotic/necrotic/healthy cells detection kit to differentiate the status of the cells. All scale bars represent 200 μm.

to 6), only the emission from Hoechst staining (blue) was seen. This confirms that the cells are healthy and that the PA particles are not toxic. For the azTM treated cells, the Hoechst staining (cf. Figure 10 - panel 7) indicated that the number of healthy cells decreased by ca. 38 % which was coupled with a decrease in the intensity of the blue emission, suggesting the possibility of DNA damage. In addition, the emission was not a normal bright round spot but appeared to be shaped like clumped random strands. It was subsequently verified that this blue emission from random strand like shapes was attributed to the emission of the azTM and not the Hoechst dye. The azTM treated cells indicated ca. 43 % apoptotic cell death and the images obtained (cf. Figure 10 - panels 7 to 9) suggested that the cells were in the late apoptotic stage, as they were stained by all the three dyes (blue, green and red). When cells are stained with the triple colors blue, green, and red, this indicates that those cells are dead cells progressing from apoptotic cell population [53,54]. For the treatment of PA/ azTM particles with a grafting density of 0.63 azTM/ nm^2 (cf. Figure 10 - panels 10 to 12), ca. 66 % reduction in healthy cells was observed and the late apoptotic cell population was ca. 18 %. In this treatment, the apoptotic cell death was lower than expected, which could be due to a loss of dead cells during the wash with buffer prior to the staining process. For treatments with particles of higher grafting density of azTM/nm^2 (cf. Figure 10 - panels 13 and 16), the number of healthy cells was not reduced when compared to the controls (cf. Figure 10 - panels 1 and 4), suggesting that the high azTM grafting density particles were not that effective. This result is in accordance with the earlier speculation that particles with higher grafting densities of the ligands did not allow the proteins the spatial flexibility to bind (cf. Figure 8). In addition, there is a ca. 30 to 40 % decrease in the number of late apoptotic cells for treatment with the PEGylated particles (cf. Figure 10 - panel 17) when compared to non-PEGylated particles (cf. Figure 10 - panel 14), which also supports the previous speculation that protein transport to the surface of the particles is reduced with a large PEG hydration shell.

4 Conclusion

Disrupting the activity of anti-apoptotic proteins that are over-expressed by cancer cells is a potentially attractive route to combating this disease. Survivin belongs to the family of inhibitor of apoptosis proteins (IAP) and is present in most cancers while being below detection limits in most terminally differentiated adult tissues, making it an attractive protein to target for diagnostic and, potentially, therapeutic roles. To this end, sub-100 nm poly(propargyl acrylate) particles were surface modified through the copper-catalyzed azide/alkyne cycloaddition of an azide-terminated survivin ligand derivative (azTM) originally proposed by Abbott Labs and speculated to bind directly to survivin (protein) at its dimer interface. Using affinity pull-down studies, it was determined that the PA/azTM nanoparticles selectively bind survivin. Incubating the modified particles with glioblastomas and other survivin over-expressing cell lines such as A549 and MCF7 resulted in a higher percentage of cell death relative to cells incubated with the original Abbott-derived small molecule. In situ Wright staining and selective dyes were used to confirm that the cell death observed was through apoptosis. In addition, a Western blot assay indicated that there was an significant increase in the expression of caspase-3, the final executioner of apoptosis, during the treatment with the PA/azTM particles. These particles offer a flexible platform that can be easily surface modified to recursively attach a range of moieties such as near infrared fluorophores, antibodies, and drugs to one particle, creating a multifunctional nanodevice for use against cancer.

Acknowledgments

The authors thank the National Science Foundation (DMR-1507266), the Gregg-Graniteville Foundation, and the National Institutes of Health (GM098510) for financial support.

Keywords

Survivin, targeting, nanoparticles, apoptosis, protein

References

1 D. C. Altieri, *Nature Reviews Cancer*, 2008, **8**, 61–70.
2 F. Z. Li, G. Ambrosini, E. Y. Chu, J. Plescia, S. Tognin, P. C. Marchisio and D. C. Altieri, *Nature*, 1998, **396**, 580–584.
3 C. Adida, P. L. Crotty, J. McGrath, D. Berrebi, J. Diebold and D. C. Altieri, *American Journal of Pathology*, 1998, **152**, 43–49.

This journal is © The Royal Society of Chemistry [year]

4 G. Ambrosini, C. Adida and D. C. Altieri, *Nature Medicine*, 1997, **3**, 917–921.

5 D. C. Altieri, *Nature Reviews Cancer*, 2003, **3**, 46–54.

6 D. C. Altieri, *Oncogene*, 2003, **22**, 8581–8589.

7 S. Fukuda and L. M. Pelus, *Molecular Cancer Therapeutics*, 2006, **5**, 1087–1098.

8 J. George, N. L. Banik and S. K. Ray, *Neuro-Oncology*, 2010, **12**, 1088–1101.

9 I. Fraunholz, C. Rodel, L. Distel, M. Rave-Frank, D. Kohler, S. Falk and F. Rodel, *Radiation Oncology*, 2012, **7**, year.

10 S. M. Kennedy, L. O'Driscoll, R. Purcell, N. Fitz-simons, E. W. McDermott, A. D. Hill, N. J. O'Higgins, M. Parkinson, R. Linehan and M. Clynes, *British Journal of Cancer*, 2003, **88**, 1077–1083.

11 Y. G. Lv, F. Yu, Q. Yao, J. H. Chen and L. Wang, *Journal of thoracic disease*, 2010, **2**, year.

12 H. Yamamoto, C. Y. Ngan and M. Monden, *Cancer Science*, 2008, **99**, 1709–1714.

13 M. E. Johnson and E. W. Howerth, *Veterinary Pathology*, 2004, **41**, 599–607.

14 S. Shin, B. J. Sung, Y. S. Cho, H. J. Kim, N. C. Ha, J. I. Hwang, C. W. Chung, Y. K. Jung and B. H. Oh, *Biochemistry*, 2001, **40**, 1117–1123.

15 J. Drappatz, A. D. Norden and P. Y. Wen, *Expert review of neurotherapeutics*, 2009, **9**, year.

16 S. Fulda and K. M. Debatin, *Oncogene*, 2006, **25**, 4798–4811.

17 C. S. Straub, *Current Topics in Medicinal Chemistry*, 2011, **11**, 291–316.

18 M. S. Coumar, F. Y. Tsai, J. R. Kanwar, S. Sarvagalla and C. H. A. Cheung, *Cancer Treatment Reviews*, **39**, 802–811.

19 D. C. Talbot, M. Ranson, J. Davies, M. Lahn, S. Callies, V. Andre, S. Kadam, M. Burgess, C. Slapak, A. L. Olsen, P. J. McHugh, J. S. de Bono, J. Matthews, A. Saleem and P. Price, *Clinical Cancer Research*, 2010, **16**, 6150–6158.

20 P. Sapra, M. L. Wang, R. Bandaru, H. Zhao, L. M. Greenberger and I. D. Horak, *Nucleosides Nucleotides & Nucleic Acids*, 2010, **29**, 97–112.

21 D. Mahalingam, E. C. Medina, J. A. Esquivel, C. M. Espitia, S. Smith, K. Oberheu, R. Swords, K. R. Kelly, M. M. Mita, A. C. Mita, J. S. Carew, F. J. Giles and S. T. Nawrocki, *Clinical Cancer Research*, 2010, **16**, 141–153.

22 R. A. Olie, A. P. Simoes-Wust, B. Baumann, S. H. Leech, D. Fabbro, R. A. Stahel and U. Zangemeister-Wittke, *Cancer Research*, 2000, **60**, 2805–2809.

23 D. J. Dai, C. D. Lu, R. Y. Lai, J. M. Guo, H. Meng, W. S. Chen and J. Gu, *World Journal of Gastroenterology*, 2005, **11**, 193–199.

24 R. A. Carrasco, N. B. Stamm, E. Marcusson, G. Sandusky, P. Iversen and B. K. R. Patel, *Molecular Cancer Therapeutics*, 2011, **10**, 221–232.

25 S. Callies, V. Andre, B. Patel, D. Waters, P. Francis, M. Burgess and M. Lahn, *British Journal of Clinical Pharmacology*, 2011, **71**, 416–428.

26 J. B. Hansen, N. Fisker, M. Westergaard, L. S. Kjaerulff, H. F. Hansen, C. A. Thrue, C. Rosenbohm, M. Wissenbach, H. Orum and T. Koch, *Molecular Cancer Therapeutics*, 2008, **7**, 2736–2745.

27 K. Yamanaka, T. Nakahara, T. Yamauchi, A. Kita, M. Takeuchi, F. Kiyonaga, N. Kaneko and M. Sasamata, *Clinical Cancer Research*, 2011, **17**, 5423–5431.

28 T. Nakahara, M. Takeuchi, I. Kinoyama, T. Minematsu, K. Shirasuna, A. Matsuhisa, A. Kita, F. Tominaga, K. Yamanaka, M. Kudoh and M. Sasamata, *Cancer Research*, 2007, **67**, 8014–8021.

29 Q. Cheng, X. Ling, A. Haller, T. Nakahara, K. Yamanaka, A. Kita, H. Koutoku, M. Takeuchi, M. G. Brattain and F. Li, *International journal of biochemistry and molecular biology*, 2012, **3**, year.

30 X. Ling, S. S. Cao, Q. Y. Cheng, J. T. Keefe, Y. M. Rustum and F. Z. Li, *Plos One*, **7**, 18.

31 V. Pisarev, B. Yu, R. Salup, S. Sherman, D. C. Altieri and D. I. Gabrilovich, *Clinical Cancer Research*, 2003, **9**, 6523–6533.

32 S. Siegel, A. Wagner, N. Schmitz and M. Zeis, *British Journal of Haematology*, 2003, **122**, 911–914.

33 M. D. Wendt, C. H. Sun, A. Kunzer, D. Sauer, K. Sarris, E. Hoff, L. P. Yu, D. G. Nettesheim, J. Chen, S. Jin, K. M. Comess, Y. H. Fan, S. N. Anderson, B. Isaac, E. T. Olejniczak, P. J. Hajduk, S. H. Rosenberg and S. W. Elmore, *Bioorganic & Medicinal Chemistry Letters*, 2007, **17**, 3122–3129.

34 T. Oikawa, Y. Unno, K. Matsuno, J. Sawada, N. Ogo, K. Tanaka and A. Asai, *Biochemical and Biophysical Research Communications*, 2010, **393**, 253–258.

35 N. Zaffaroni, M. Pennati and M. G. Daidone, *Journal of Cellular and Molecular Medicine*, 2005, **9**, 360–372.

36 C. F. Bennett and E. E. Swayze, *Annual Review of Pharmacology and Toxicology*, 2010, **50**, 259–293.

37 K. D. Lewis, W. Samlowski, J. Ward, J. Catlett, L. Cranmer, J. Kirkwood, D. Lawson, E. Whitman and R. Gonzalez, *Investigational New Drugs*, 2011, **29**, 161–166.

38 G. Giaccone, P. Zatloukal, J. Roubec, K. Floor, J. Musil, M. Kuta, R. J. van Klaveren, S. Chaudhary, A. Gunther and S. Shamsili, *Journal of Clinical Oncology*, 2009, **27**, 4481–4486.

39 M. Mobahat, A. Narendran and K. Riabowol, *International Journal of Molecular Sciences*, 2014, **15**, 2494–2516.

40 A. Berezov, Z. Cai, J. A. Freudenberg, H. Zhang, X. Cheng, T. Thompson, R. Murali, M. I. Greene and Q. Wang, *Oncogene*, **31**, 1938–1948.

41 Y. G. Shi, *Nature Structural Biology*, 2000, **7**, 620–623.

42 H. Guvenc, M. S. Pavlyukov, K. Joshi, H. Kurt, Y. K. Banasavadi-Siddegowda, P. Mao, C. Hong, R. Yamada, C. H. Kwon, D. Bhasin, S. Chettiar, G. Kitange, I. H. Park, J. N. Sarkaria, C. L. Li, M. I. Shakhparonov and I. Nakano, *Clinical Cancer Research*, 2013, **19**, 631–642.

43 F. Xia, P. M. Canovas, T. M. Guadagno and D. C. Altieri, *Molecular and Cellular Biology*, 2008, **28**, 5299–5311.

44 M. K. Yu, J. Park and S. Jon, *Theranostics*, 2012, **2**, 3–44.

45 R. Weissleder, K. Kelly, E. Y. Sun, T. Shtatland and L. Joseph-

son, *Nature Biotechnology*, 2005, **23**, 1418–1423.
46 A. V. Ullal, T. Reiner, K. S. Yang, R. Gorbatov, C. Min, D. Issadore, H. Lee and R. Weissleder, *Acs Nano*, 2011, **5**, 9216–9224.
47 C. Tassa, J. L. Duffner, T. A. Lewis, R. Weissleder, S. L. Schreiber, A. N. Koehler and S. Y. Shaw, *Bioconjugate Chemistry*, 2009, **21**, 14–19.
48 S. Hong, P. R. Leroueil, I. J. Majoros, B. G. Orr, J. R. Baker Jr and M. M. Banaszak Holl, *Chemistry & Biology*, 2007, **14**, 107–115.
49 J. B. Haun, N. K. Devaraj, S. A. Hilderbrand, H. Lee and R. Weissleder, *Nature Nanotechnology*, 2010, **5**, 660–665.
50 A. H. Abadi, D. A. Abouel-Ella, J. Lehmann, H. N. Tinsley, B. D. Gary, G. A. Piazza and M. A. O. Abdel-Fattah, *European Journal of Medicinal Chemistry*, 2010, **45**, 90–97.
51 A. Abadi, O. Al-Deeb, A. Al-Afify and H. El-Kashef, *Il Farmaco*, 1999, **54**, 195–201.
52 P. Rungta, Y. P. Bandera, M. G. Sehorn and S. H. Foulger, *Macromolecular Bioscience*, 2011, **11**, 927–937.
53 E. Szliszka, Z. P. Czuba, K. Jernas and W. Krol, *International Journal of Molecular Sciences*, 2008, **9**, 56–64.
54 J. Bronikowska, E. Szliszka, Z. P. Czuba, D. Zwolinski, D. Szmydki and W. Krol, *Molecules*, 2010, **15**, 2000–2015.
55 I. H. Park and C. L. Li, *Journal of Physical Chemistry B*, 2010, **114**, 5144–5153.
56 A. H. Abadi, T. M. Ibrahim, K. M. Abouzid, J. Lehmann, H. N. Tinsley, B. D. Gary and G. A. Piazza, *Bioorganic & Medicinal Chemistry*, 2009, **17**, 5974–5982.
57 A. H. Abadi, M. S. Hany, S. A. Elsharif, A. A. H. Eissa, B. D. Gary, H. N. Tinsley and G. A. Piazza, *Chemical & Pharmaceutical Bulletin*, **61**, 405–410.
58 R. Janardhanan, N. L. Banik and S. K. Ray, *Biochemical Pharmacology*, 2009, **78**, 1105–1114.
59 S. N. Chettiar, J. V. Cooley, I. H. Park, D. Bhasin, A. Chakravarti, P. K. Li, C. L. Li and N. K. Jacob, *Bioorganic & Medicinal Chemistry Letters*, **23**, 5429–5433.
60 P. Sur, E. A. Sribnick, J. M. Wingrave, M. W. Nowak, S. K. Ray and N. L. Banik, *Brain Research*, 2003, **971**, 178–188.
61 S. K. Ray, S. Karmakar, M. W. Nowak and N. L. Banik, *Neuroscience*, 2006, **139**, 577–595.
62 J. J. Liu, R. W. Huang, D. J. Lin, J. Peng, X. Y. Wu, Q. Lin, X. L. Pan, Y. Q. Song, M. H. Zhang, M. Hou and F. Chen, *Annals of Oncology*, 2005, **16**, 455–459.
63 J. D. Lickliter, N. J. Wood, L. Johnson, G. McHugh, J. Tan, F. Wood, J. Cox and N. W. Wickham, *Leukemia*, 2003, **17**, 2074–2080.
64 S. Karmakar, M. S. Weinberg, N. L. Banik, S. J. Patel and S. K. Ray, *Neuroscience*, 2006, **141**, 1265–1280.
65 A. Das, N. L. Banik and S. K. Ray, *Cancer*, 2007, **110**, 1083–1095.
66 H. N. Zhen, L. W. Li, W. Zhang, Z. Fei, C. H. Shi, T. T. Yang, W. T. Bai and X. Zhang, *International Journal of Oncology*, 2007, **31**, 1111–1117.
67 R. Jetty, Y. P. Bandera, M. A. Daniele, D. Hanor, H. I. Hung, V. Ramshesh, M. F. Duperreault, A. L. Nieminen, J. J. Lemasters and S. H. Foulger, *Journal of Materials Chemistry B*, 2013, **1**, 4542–4554.
68 S. M. Moghimi, A. C. Hunter and J. C. Murray, *Pharmacological Reviews*, 2001, **53**, 283–318.
69 I. Tamm, Y. Wang, E. Sausville, D. A. Scudiero, N. Vigna, T. Oltersdorf and J. C. Reed, *Cancer Research*, 1998, **58**, 5315–5320.
70 M. Lieber, B. Smith, A. Szakal, W. Nelsonrees and G. Todaro, *International Journal of Cancer*, 1976, **17**, 62–70.
71 A. L. Klibanov, K. Maruyama, V. P. Torchilin and L. Huang, *Febs Letters*, 1990, **268**, 235–237.
72 V. P. Torchilin, A. L. Klibanov, L. Huang, S. Odonnell, N. D. Nossiff and B. A. Khaw, *Faseb Journal*, 1992, **6**, 2716–2719.
73 M. Vittaz, D. Bazile, G. Spenlehauer, T. Verrecchia, M. Veillard, F. Puisieux and D. Labarre, *Biomaterials*, 1996, **17**, 1575–1581.
74 F. De Jaeghere, E. Allemann, J. Feijen, T. Kissel, E. Doelker and R. Gurny, *Journal of Drug Targeting*, 2000, **8**, 143–153.
75 F. Belloc, P. Dumain, M. R. Boisseau, C. Jalloustre, J. Reiffers, P. Bernard and F. Lacombe, *Cytometry*, 1994, **17**, 59–65.
76 C. F. Brunk, K. C. Jones and T. W. James, *Analytical Biochemistry*, 1979, **92**, 497–500.
77 H. A. Crissman, M. E. Wilder and R. A. Tobey, *Cancer Research*, 1988, **48**, 5742–5746.
78 H. M. Shapiro, *Cytometry*, 1981, **2**, 143–150.
79 S. J. Martin, C. P. M. Reutelingsperger, A. J. McGahon, J. A. Rader, R. Vanschie, D. M. Laface and D. R. Green, *Journal of Experimental Medicine*, 1995, **182**, 1545–1556.
80 I. Vermes, C. Haanen, H. Steffensnakken and C. Reutelingsperger, *Journal of Immunological Methods*, 1995, **184**, 39–51.
81 A. W. M. Boersma, K. Nooter, R. G. Oostrum and G. Stoter, *Cytometry*, 1996, **24**, 123–130.
82 J. M. Laing, M. D. Gober, E. K. Golembewski, S. M. Thompson, K. A. Gyure, P. J. Yarowsky and L. Aurelian, *Molecular Therapy*, 2006, **13**, 870–881.
83 E. Tuite and B. Norden, *Bioorganic & Medicinal Chemistry*, 1995, **3**, 701–711.

This journal is © The Royal Society of Chemistry [year]

particles surface-functionalized
with Survivin ligand

survivin ligand